physica status solidi pss a
www.pss-a.com

Influence of Cosolvents on the Pressure Stability of Human Serum Albumin

Jaqueline Savelkouls, Eric Schneider, Chang Hee Woo, and Michael Paulus*

A small-angle X-ray scattering study on the pressure-dependent behavior of human serum albumin (HSA) is presented. HSA is able to absorb cosolvents such as drugs or other hydrophobic substances and transport them, for example, in the human body. It is shown that the uptake of various substances is associated with increased pressure stability, which can be used as an indicator of protein–substance interaction. Especially the interaction between the substances and the hydrophobic pockets of the protein is an important aspect, which mainly depends on the hydrophobicity as well as the size of the used cosolvents. Specifically, drugs such as ibuprofen and theophylline increase the pressure stability of the protein enormously, while caffeine or TMAO, for example, has no strong influence.

1. Introduction

The transport of chemicals within the human body is partly carried out by proteins that are able to form reversible bonds with them. Whether the protein can absorb an active substance depends on many factors such as hydrophobicity or the size of the active substance molecule. One protein that can perform this task is human serum albumin (HSA), which is the most common blood protein in humans. It represents around half of total plasma protein (0.6 mM or 5 g mL^{-1}[1,2]). HSA is a large globular protein with a high alpha-helix content. It contributes to osmotic colloid pressure, regulates blood pH, and acts as plasma transporter for various substances. It has the capacity to bind substances such as fatty acids, various hydrophobic steroid hormones, and drugs.[3] Due to its wide availability and biocompatibility, HSA is being discussed as a nanocontainer for medicine in the context of specific applications (see, for example, refs. [4–7]). HSA has a mass of 66.5 kDa and is present at pH 7 in a heart-shaped form. The isoelectric point of HSA is pH 4.6, i.e., it is positively charged at pH 7. The radius of gyration of HSA is 2.8 nm. Studies mainly focus on the binding of fatty acids to HSA indicate that HSA has up to eight binding sites that can interact with fatty acids to varying degrees.[8,9] However, it might be difficult to provide direct evidence of the uptake of active substances, for example, using structure-determining methods such as small-angle X-ray scattering (SAXS), because the molecules can be very small compared to the protein and structural changes in a disordered system such as protein solutions cannot be adequately resolved. Here, an indirect proof of the interaction between protein and active substance might be possible, for example, via the denaturation behavior of proteins.

In addition to thermal denaturation and denaturation by extreme chemical environments (pH, salt, and cosolvents), the application of high hydrostatic pressure is a method that can move proteins out of their native, folded state. The application of high pressure in the range of a few kbar still represents a relatively mild disruption of the proteins, which is not sufficient to destroy covalent bonds, see, for example, refs. [10,11]. Furthermore, high pressure can be used to produce protein nanoparticles (in the case of HSA, for example, the drug Abraxane) by forming an active ingredient cluster inside a shell of proteins that are not completely denatured.[12]

Proteins under pressure tend to minimize their intrinsic volume, which can happen quite reversibly. Structural changes, for example, through mutation,[13] changes in the structure of the solvent[14] as well as the docking of molecules, can have a strong effect on the pressure stability of individual proteins. In the case of HSA, it has been shown that the uptake of fatty acids significantly increases the protein's stability against high hydrostatic pressures.[15] This change in the pressure-dependent behavior of HSA is to be used in this work to investigate the interaction of various substances with the protein. To this end, the influence of the fatty acid heptanoic acid, the drugs theophylline and ibuprofen, the nucleic base uracil, the biogenic amine histamine, caffeine, the complex compound hemin, and the osmolyte trimethylaminoxide (TMAO) on the pressure stability of the HSA was investigated. The stability of the protein was analyzed using SAXS at the DELTA (Dortmund Electron Accelerator) synchrotron radiation source. It is shown that all used substances interact with the fatty acid-free HSA and influence the pressure stability of the protein. However, the strength of the stabilization effect varies significantly depending on the individual molecules used.

J. Savelkouls, E. Schneider, C. H. Woo, M. Paulus
Fakultät Physik/DELTA
TU Dortmund
44221 Dortmund, Germany
E-mail: jaqueline.savelkouls@tu-dortmund.de

The ORCID identification number(s) for the author(s) of this article can be found under https://doi.org/10.1002/pssa.202400608.

This paper was presented at EMRS spring meeting 2024.

DOI: 10.1002/pssa.202400608

1.1. SAXS

SAXS[16] is an established method for characterizing the shape, size, and interactions of nanoscale objects such as colloids, polymers, or proteins. The objects can be disordered, for example, in an aqueous solution. In a SAXS experiment, a monochromatic X-ray beam hits a sample and is elastically scattered under small angles 2θ which are in the range of a few degrees. In the case of highly dilute solutions, where the individual particles do not interact with each other, the scattered intensity $I(q)$ as a function of the wave vector transfer $q = 4\pi/\lambda \sin(\theta)$, with the wavelength λ of the used radiation, is described by the so-called form factor $P(q)$ of the scattering object:

$$I(q) \propto P(q) = <|F(\vec{q})|^2>_\Omega \tag{1}$$

with the scattering amplitude $F(\vec{q})$, which is the Fourier transform of the particles electron density $\rho(r)$. Here, $<..>_\Omega$ stands for the average over all particle orientations and positions. For small q, the scattered intensity of a monodisperse system can be described in the so-called Guinier approximation given by

$$I(q) \approx I(q=0) \times e^{-q^2 \times R_G^2/3} \tag{2}$$

with the radius of gyration R_G of the particles[17]

$$R_G^2 = \frac{\int \rho(r) r^2 d^3 r}{2 \int \rho(r) d^3 r} \tag{3}$$

which describes the mean electronic extent of the scattering particle. Thus, plotting $\ln(I(q))$ versus q^2 can be used for a simple determination of the particles' size. Note that this approximation is only valid in the q - region where $q \times R_G < 1.3$ holds.[17] Another approach to determine among others the size of the scattering object, which was used to validate the results, is to adjust the distance distribution function $p(r)$,[18] which is connected to the scattered intensity $I(q)$ via

$$p(r) = \frac{1}{2\pi^2} \int_0^\infty I(q) q r \sin(qr) dq \tag{4}$$

This approach is implemented in the ATSAS program package,[19] for example, and uses the entire q range of the measured data for the analysis.

2. Experimental Section

The SAXS measurements were carried out at the beamline BL2[20] of the DELTA synchrotron radiation source in Dortmund.[21] DELTA is a 1.5 GeV electron storage ring in which a maximum electron current of 130 mA is stored with a lifetime of ≈30 h at 100 mA. The beamline is built at a 1.5 T bending magnet with a critical energy of 2.1 keV. A multilayer monochromator monochromatizes the incident polychromatic X-ray radiation to an energy of 12 keV within a bandwidth of 1.5%. The beam size of the collimated beam at the sample location is 0.5×0.5 mm^2. The pressure cell[22] consists of a cubic inconel steel block with an edge length of 10 cm. The cell has three large openings with fine threads. Two of them are located opposite each other and are closed by special plugs, each of which has a 1 mm thick diamond window. These windows have sufficient transmission at a photon energy of 12 keV and can withstand a cell pressure of up to 5000 bar. The third opening is for changing samples and can be closed by a plug. At the rear of the cell, there is a connection for 6 mm thick high-pressure pipes through which water can be pumped into the interior of the cell. This allows the pressure inside the cell to be varied between 50 and 4000 bar using a spindle pump (Sitec, Switzerland). The pressure can be measured by two pressure sensors. To separate the sample to be analyzed from the water flowing into the cell, the sample is filled into a separate small sample holder with a volume of ≈0.2 mL. The sample holder has two flexible polyimide windows, which transfer the adjacent pressures to the inside of the sample holder. The outer cell body is drilled with several holes through which water can be pumped to control the temperature of the cell. The cell is connected to a 1.5 m long evacuated flightpath, which has a polyimide entrance window with a diameter of 10 mm. At the end, the flightpath has another polyimide window with a diameter of 25 cm and 0.125 mm thickness. As detector, a MAR345 imageplate (marXperts, Norderstedt, Germany) is used. To intercept the transmitted X-ray beam, a lead beam stopper is located in front of the detector and in direct contact with the exit window of the flight path.

Fatty acid-free HSA (Sigma-Aldrich) was used to analyze the substance that was uptaken by HSA. The HSA was mixed at a concentration of 10 mg mL^{-1} in pressure-stable Bis-Tris buffer (25 mM, Sigma-Aldrich). The different cosolvents were added during preparation at the concentrations listed in **Table 1**. The fresh samples were then filled into sample holders and transferred directly into the high-pressure cell. All pressure-dependent SAXS measurements were carried out at a temperature of 25 °C. After closing the pressure cell, the pressure was increased in steps of 250 bar up to a final pressure of 3500 bar and SAXS images were taken with an exposure time of 300 s in each case. To determine the scattering background, data of pure buffer were recorded at the corresponding pressures. The SAXS setup was calibrated by using silver behenate (Sigma-Aldrich) as a calibration standard.

3. Analysis and Discussion

The Fit2D[23] program package was used for the azimuthal integration of the 2D SAXS data. The measurements on the silver behenate were used to precisely determine the beam position on the detector, the distance between the sample and the detector and any tilting of the experimental setup. The intensities of the pure buffer measurements were subtracted from the integrated intensities of the measurements with protein in a second step. The data generated in this way are shown as an example for two systems one consisting of fatty acid-free HSA (left) and one with fatty acids (right) in **Figure 1**. Both samples show the typical curve of a globular protein at normal pressure. The fitting in the Guinier range results in a radius of gyration of 2.9 nm for both samples, which corresponds to values found in the literature for the folded heart-shaped structure of the HSA.[24] In comparison, the radius of gyration for unfolded HSA (E-form) ranges at >3.4 nm. A detailed view of the curves at higher pressures indicates a shift in the slope around $p = 1000$ bar. At this

Table 1. An overview of the substances used in the experiment. The Chemical Abstracts Service (CAS) number is a unique numerical identifier that is assigned to a specific chemical substance.

Substance	CAS-Number	Concentration	Origin	Chemical formula	Comment
HSA A3782	70 024-90-7	10 mg/mL	Sigma-Aldrich	–	Fatty acid free
HSA A8763	70 024-90-7	10 mg/mL	Sigma-Aldrich	–	Unspecified amount of fatty acids
TMAO	62 637-93-8	50 mM	ThermoScientific	$(CH_3)_3NO$	Small, good solubility[42]
Histamine	51-45-6	50 mM	Sigma-Aldrich	$C_5H_9N_3$	Low solubility (3.4 g/100 mL)[43]
Ibuprofen	15 687-27-1	5 mM	Sigma-Aldrich	$C_{13}H_{18}O_2$	Low solubility (0.002 g/100 mL)[44]
Caffeine	58-08-2	50 mM	AlfaAesar	$C_8H_{10}N_4O_2$	Low solubility (2 g/100 mL)[45]
Hemin	16 009-13-5	100 mM	AlfaAesar	$C_{34}H_{32}ClFeN_4O_2$	Very low solubility (0.9 mg/100 mL)[46]
Uracil	66-22-8	50 mM	Roth	$C_4H_4N_2O_2$	Very low solubility (0.36 g/100 mL)[47]
Theophylline	58-55-9	50 mM	Sigma-Aldrich	$C_7H_8N_4O_2$	Very low solubility (0.8 g/100 mL)[48]
Heptanoic acid	111-14-8	2 mM	Sigma-Aldrich	$C_7H_{14}O_2$	Very low solubility (0.24 g/100 mL)[49]

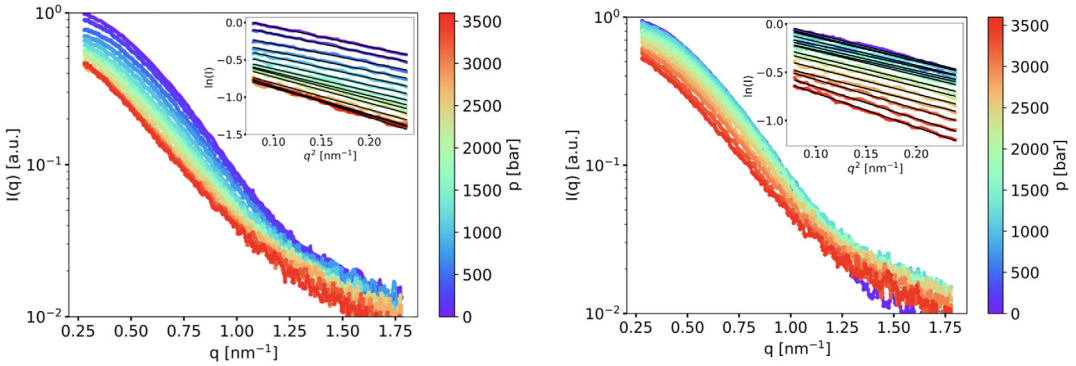

Figure 1. Pressure-dependent SAXS data of the samples HSA A3782 (left, fatty acid free) and HSA A8763 (right). The insets show the Guinier regions with corresponding fit to the data (black lines).

pressure, the entire curve loses the shape typical of globular protein. A change in the slope can also be recognized in the Guinier region, which indicates an increase in the radius of gyration. In the SAXS curves on the right-hand side in Figure 1, which originate from HSA that is not fatty acid-free, the change in curve behavior at 1000 bar does not occur. As on the left-hand side, the decrease in intensity can be recognized, which can be explained by the decrease in the scattering contrast between the protein and the compressed water phase. In the Guinier range, too, the change in the gradient of the curve cannot be seen, but rather a continuous increase in the gradient. The radius of gyration of the HSA resulting from the Guinier fits is summarized in **Figure 2**.

The radius of gyration clearly shows that the volume of the protein only changes slightly. It therefore does not appear to unfold completely, which is a typical behavior for pressure-induced unfolding.[25] At first glance, the increase in volume of the protein seems to contradict the postulate that predicts a decrease in volume when pressure is increased. However, it should be noted that the entire system consisting of protein and solvent must be considered here. The protein is a complex structure which often contains hydrophobic cavities in the inner core which are not accessible to the solvent. The hydrophobic cavities have a size of ≈16 Å in depth and about 8 Å in width.[26] Only under a significant increase in pressure can these cavities be filled by penetrating solvent molecules.[27] Among other things, this effect leads to a reduction in the total volume of the system when the pressure is increased.[25] When fatty acids are added to the HSA solvent system, the hydrophilic headgroups interact with the polar groups of the protein, which are located on the protein surface and especially at the entrances of the binding pockets, while the hydrophobic parts of the fatty acids fill the interior of the pockets and interact with hydrophobic side chains.[28] We conclude that the filling of these pockets counteracts the pressure-induced unfolding by reducing the free volume occupied by the solvent when the pressure is increased. Another factor for stabilization could be the energetically unfavorable rehydration of the hydrophobic fatty acid chains, which would have to be accepted if the protein were to unfold. However, to the best of our knowledge, there is no precise description of the pressure-induced interaction mechanisms between the fatty acids and the protein.

The pressures at which an increase in the radius of gyration was observed were determined for all substances used and are summarized in **Table 2**. It is clear that all substances have a stabilizing effect against the applied pressure, albeit to very different

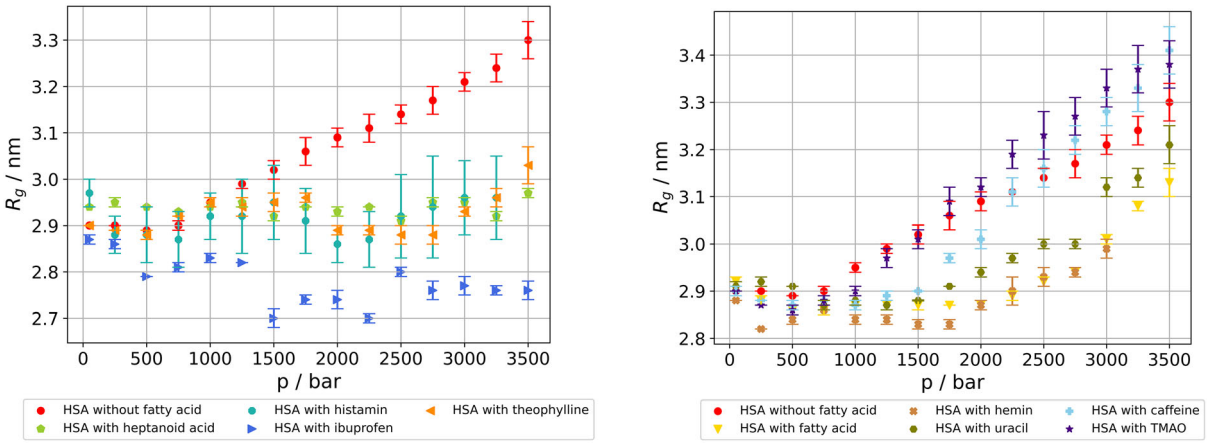

Figure 2. The radius of gyration of HSA A3782, which has uptaken strong stabilizers (left) and average as well weak stabilizers (right). The radius of gyration was determined with the aid of Guinier fits.

Table 2. Pressures (given in bar) under which denaturation of HSA starts.

HSA A3782	HSA A8763	Caffeine	Hemin	Histamine	Heptanoic acid	Uracil	Theophylline	Ibuprofen	TMAO
1000 bar	2500 bar	1500 bar	2250 bar	>3250 bar	>3500 bar	2750 bar	3250 bar	>3500 bar	1250 bar

degrees. The substances can be roughly categorized into three groups. The first group consists of strong stabilizers such as heptanoic acid, ibuprofen, theophylline, and histamine, which raise the denaturation pressure above 3000 bar and therefore have a stronger effect in the concentrations used than the fatty acids naturally present in HSA A8763, the average stabilizers such as uracil and hemin, which raise the denaturation pressure to between 2250 and 2750 bar, and the weak stabilizers such as caffeine and TMAO, which only raise the denaturation pressure by a few hundred bar. A special role is played here by TMAO with approximate dimensions of 11 Å in length and width,[29] which generally stabilizes proteins due to its water-stabilizing properties.[30] It is therefore doubtful whether the slight increase in denaturation pressure of HSA is caused by a specific interaction between HSA and TMAO. It is noticeable that especially those substances with a low water solubility have a strong stabilizing effect, which can be explained by their strong hydrophobicity. The interaction of the hydrophobic molecules with the hydrophobic side chains inside the protein thus appears to be an important factor in the stabilization of HSA. However, hemin does not seem to follow this trend with its extremely low water solubility. This can be explained by the geometry of the molecule. Compared to the other substances used, hemin is a relatively large molecule that forms flat platelets. As a result, only a few binding pockets can be occupied by the hemin[28] and thus the penetration of water molecules into the protein core can be prevented to a lesser extent. Similar to hemin, the nucleic base uracil can also be classified as a weak stabilizer. Uracil has a very low water solubility and can interact with the hydrophobic pockets of the protein through its hydrophobic pyrimidine ring.[31] However, this interaction does not appear to be strong enough to stabilize the protein above 2750 bar. This is also supported by the measurements on caffeine, which also contains a pyrimidine ring which does not significantly stabilize the protein under pressure. The binding affinity between caffeine and the hydrophobic pockets of HSA appears to be very low.[32] However, some studies generally indicate a high binding affinity of caffeine on HSA.[33] Caffeine has a length of ≈7 Å and a width of ≈15 Å.[34] Based on the low influence on the pressure stability and the size of the caffeine molecule, we assume that the caffeine molecule interacts with other sites of the protein and less with the hydrophobic pockets. Compared to the previous substances, the fatty acid heptanoic acid is an ingredient in which the protein structure remains stable over the pressure range. The fatty acid is ≈10 Å in length and ≈5 Å in width.[35] It can settle in the hydrophobic pockets of the HSA, where it interacts with the protein via hydrophobic interactions. This fills the cavity volume so that the protein structure is not affected by an increase in pressure. Furthermore, the drugs ibuprofen and theophylline stabilize the HSA structure extremely well, too. These observations confirm previous research results that have found a strong affinity between the drugs and the protein.[36,37] According to previous studies, ibuprofen, which has a length of ≈11 Å and a width of ≈7 Å,[38] binds to the hydrophobic tyrosyl and tryptophan residues of the HSA,[37] which means that a complete occupancy of the inner pockets can be assumed. In addition, the tryptophan–tryptophan hydrogen bonds are dissolved during binding, which is why hydrophobic tryptophan chains may be present in the remaining cavities.[37] It has been suggested that the volume of the remaining cavities is so small that no penetration of water molecules into the protein core can occur under increased pressure. This has been confirmed by the fact that the protein structure is stable over the entire measurement range. The slightly smaller drug theophylline, with a length of ≈8 Å and a width

of ≈4 Å,[39] also exhibits a high stabilization rate, which can be attributed to its extremely strong hydrophobicity resulting in strong hydrophobic interactions inside HSA. Compared to the other strong stabilizers, histamine has a lower hydrophobicity. However, with a length of around 14 Å and a width of ≈16 Å,[40] histamine is significantly larger than the other strongly stabilizing molecules. Nevertheless, histamine has a good binding affinity to HSA, which is illustrated by its high-pressure stability. It is already known that histamine interacts with the hydrophobic lysine residue of the protein via a hydrogen bond.[41] In this way, the interaction of histamine with the hydrophobic protein core may stabilize the structure of HSA.

4. Conclusion

In summary, all substances have a varying degree of influence on the pressure stability of the structure of HSA which means that an interaction between the protein and the substances could be demonstrated. Especially smaller drug molecules such as ibuprofen and theophylline induced a high-pressure stability and accordingly showed a high binding affinity to the protein. An important factor here appears to be the strength of the hydrophobicity of the molecule. In addition, the size and geometry of the substances also play a role in pressure stability, as can be seen from the hemin measurements. As a result, the interaction between the substances and the hydrophobic pockets of the protein is decisive for the pressure stability. The molecules prevent the water from penetrating into the interior of the protein when the pressure increases, thus preventing the pressure-induced unfolding of the protein. In the context of drug carrier development, increased pressure stability represents an opportunity to produce protein–drug complexes using high-pressure processes without denaturing the proteins. This would have the advantage that the full biological functionality of the proteins and thus possibly a better tolerability of the carrier are maintained.

Acknowledgements

The authors acknowledge the DELTA (Dortmund Electron Accelerator) machine group for providing synchrotron radiation and for technical support. This research project is financed through the Technical University of Dortmund.

Conflict of Interest

The authors declare no conflict of interest.

Data Availability Statement

The data that support the findings of this study are available from the corresponding author upon reasonable request.

Keywords

high hydrostatic pressures, human serum albumin, small-angle X-ray scattering

Received: July 31, 2024
Revised: October 1, 2024
Published online: November 4, 2024

[1] D. C. Carter, J. X. Ho, *Adv. Protein Chem.* **1994**, *45*, 153.
[2] T. Peters Jr., *Adv. Protein Chem.* **1985**, *37*, 161.
[3] S. Curry, P. Brick, N. P. Franks, *Biochim. Biophys. Acta* **1999**, *1441*, 131.
[4] M. Paul, A. M. Itoo, B. Ghosh, S. Biswas, *Expert Opin. Drug Delivery* **2022**, *19*, 1449.
[5] C. Li, D. Zhang, Y. Pan, B. Chen, *Polymers* **2023**, *15*, 3354.
[6] J. Wasko, M. Wolszczak, Z. Zajaczkowska, M. Dudek, B. Kolesinska, *Bioorg. Chem.* **2024**, *143*, 107104.
[7] D. Shastri, V. Raj, S. Lee, *Ageing Res. Rev.* **2024**, *99*, 102379.
[8] S. De Felice, Z. Romanyuk, M. Chinellato, G. Zoia, S. Linciano, Y. Kumada, E. Pardon, J. Steyaert, A. Angelini, L. Cendron, *Protein Sci.* **2024**, *33*, e4887.
[9] S. Linciano, G. Moro, A. Zorzi, A. Angelini, *J. Controlled Release* **2022**, *348*, 115.
[10] A. Kamali, N. Jahmidi-Azizi, R. Oliva, R. Winter, *Phys. Chem. Chem. Phys.* **2022**, *24*, 17966.
[11] H. Hata, M. Nishiyama, A. Kitao, *Biochim. Biophys. Acta, Gen. Subj.* **2020**, *1864*, 129395.
[12] J. Kaltbeitzel, P. R. Wich, *Angew. Chem., Int. Ed.* **2023**, *62*, 202216097.
[13] R. Kitahara, K. Hata, A. Maeno, K. Akasaka, M. Chimenti, B. E. Garcia-Moreno, M. A. Schroer, C. Jeworrek, M. Tolan, R. Winter, J. Roche, C. Roumestand, K. M. de Guillen, C. A. Royer, *Proteins: Struct., Funct., Bioinf.* **2011**, *79*, 1293.
[14] M. A. Schroer, Y. Zhai, D. C. F. Wieland, C. J. Sahle, J. Nase, M. Paulus, M. Tolan, R. Winter, *Angew. Chem. Int.* **2011**, *50*, 11413.
[15] Z. Toleikis, P. Cimmperman, V. Petrauskas, D. Matulis, *J. Chem. Thermodyn.* **2012**, *52*, 24.
[16] A. Guinier, *Ann. Phys.* **1939**, *12*, 237.
[17] A. Guinier, G. Fournet, *Small-Angle Scattering of X-Rays*, John Wiley & Sons, New York **1955**.
[18] O. Glatter, *Neutrons, X-ray and Light: Scattering Methods Applied to Soft Condensed Matter, Chapter 4*, 1st ed., (Eds: P. Lindner, T. Zemb), Elsevier, Amsterdam **2002**, pp. 73–102.
[19] K. Manalastas-Cantos, P. V. Konarev, N. R. Hajizadeh, A. G. Kikhney, M. V. Petoukhov, D. S. Molodenskiy, A. Panjkovich, H. D. T. Mertens, A. Gruzinov, C. Borges, C. M. Jeffries, D. I. Svergun, D. Franke, *J. Appl. Cryst.* **2021**, *54*, 343.
[20] M. Dargasz, J. Bolle, A. Faulstich, E. Schneider, M. Kowalski, C. Sternemann, J. Savelkouls, B. Murphy, M. Paulus, *J. Phys. Conf. Ser.* **2022**, *2380*, 012031.
[21] M. Tolan, T. Weis, C. Westphal, K. Wille, *Synchrotron Radiat. News* **2003**, *16*, 9.
[22] C. Krywka, C. Sternemann, M. Paulus, M. Tolan, R. Royer, R. Winter, *ChemPhysChem* **2008**, *9*, 2809.
[23] A. P. Hammersley, *ESRF Internal Report, ESRF97HA02T, FIT2D: An Introduction and Overview*, European Synchrotron Radiation Facility (ESRF), Grenoble, France **1997**. https://www.esrf.fr/computing/scientific/FIT2D/FIT2D_INTRO/fit2d.html (accessed: October 2024).
[24] C. E. Merzougui, P. Roblin, P. Aimar, A. Venault, Y. Chang, C. Causserand, P. Bacchin, *Soft Matter* **2020**, *16*, 9964.
[25] G. Hummer, S. Garde, A. E. Garcia, M. E. Paulaitis, L. R. Pratt, *Proc. Natl. Acad. Sci.* **1998**, *95*, 1552.
[26] S. Wanwimolruk, D. J. Birkett, P. M. Brooks, *Mol. Pharmacol.* **1983**, *24*, 458.
[27] J. Roche, C. A. Royer, *J. R. Soc. Interface* **2018**, *15*, 20180244.
[28] S. Curry, *Drug Metab. Pharmacokinet.* **2009**, *24*, 342.
[29] Crystallography Open Database, TMAO, https://www.crystallography.net/cod/2001043.html (accessed: July 2024).

[30] S. S. Cho, G. Reddy, J. E. Straub, D. Thirumalai, *J. Phys. Chem. B* **2011**, *115*, 13401.
[31] A. Sulkowska, *Appl. Spectrosc.* **1997**, *51*, 428.
[32] A. Krisko, M. Kveder, S. Pecar, G. Pifata, *Croat. Chem. Acta* **2005**, *78*, 71.
[33] W. Wang, W. Zhang, Y. Duan, Y. Jiang, L. Zhang, B. Zhao, P. Tu, *Spectrochim. Acta, Part A* **2013**, *115*, 57.
[34] C. W. Lehmann, F. Stowasser, *Chemistry* **2007**, *13*, 2908.
[35] A. D. Bond, *New J. Chem.* **2004**, *28*, 104.
[36] G. Rezaei Behbehani, A. A. Saboury, S. Tahmasebi Sarvestani, M. Mohebbian, M. Payehghadr, J. Abedini, *J. Therm. Anal. Calorim.* **2010**, *102*, 793.
[37] A. Ploch-Jankowska, D. Pentak, *Pharmaceuticals* **2020**, *13*, 1424.
[38] National Center for Biotechnology Information, PubChem Compound Summary for CID 3672, Ibuprofen, PubChem, https://pubchem.ncbi.nlm.nih.gov/compound/Ibuprofen#section=Crystal-Structures (accessed: July 2024).
[39] Y. Ebisuzaki, P. D. Boyle, J. A. Smith, *Acta Crystallogr., Sect. C: Cryst. Struct. Commun.* **1997**, *53*, 777.
[40] PubChem, Histamine, https://pubchem.ncbi.nlm.nih.gov/compound/774#section=Crystal-Structures (accessed: July 2024).
[41] Z. Kalaycicoglu, *J. Sep. Sci.* **2023**, *46*, 2300391.
[42] European chemicals Agency (ECHA), TMAO, https://echa.europa.eu/registration-dossier/-/registered-dossier/25104/7/2/1#::text=TMAO%20has%20a%20molecular%20weight,L%20at%2020%20%C2%B0C (accessed: July 2024).
[43] American Chemical Society, Histamine, https://www.acs.org/molecule-of-the-week/archive/h/histamine.html (accessed: July 2024).
[44] American Chemical Society, Ibuprofen, https://www.acs.org/molecule-of-the-week/archive/i/ibuprofen.html (accessed: July 2024).
[45] International Labour Organization, Caffeine, https://web.archive.org/web/20111231030423/http://www.ilo.org/legacy/english/protection/safework/cis/products/icsc/dtasht/_icsc04/icsc0405.html (accessed: July 2024).
[46] J. Yang, L. Xiong, M. Li, J. Xiao, X. Geng, B. Wang, Q. Sun, *Nanoscale Res. Lett.* **2019**, *14*, 1931.
[47] National Center for Biotechnology Information, PubChem Compound Summary for CID 1174, Uracil, https://pubchem.ncbi.nlm.nih.gov/compound/Uracil#section=Melting-Point (accessed: July 2024).
[48] Merck, Theophylline, https://www.sigmaaldrich.com/GB/en/product/sigma/t1633 (accessed: July 2024).
[49] PubChem, Heptanoic Acid, https://pubchem.ncbi.nlm.nih.gov/compound/Heptanoic-Acid#section=Solubility (accessed: July 2024).